IEEE Robotics and Automation Letters (RAL) paper presented at the
2020 IEEE International Conference on Robotics and Automation (ICRA)
31 May - 31 August, 2020. Paris, France

A Novel End-effector Robot System Enabling to Monitor Upper-extremity Posture during Robot-aided Planar Reaching Movements

Yeji Hwang[1], Seongpung Lee[2], Jaesung Hong[2], and Jonghyun Kim[1], *Member, IEEE*

Abstract— **End-effector type robots have been popularly applied to robot-aided therapy for rehabilitation purpose. However, those robots have a key drawback for the purpose: lack of the user's posture (joint angle) information. This paper proposes a novel end-effector rehabilitation robot system that contains a contactless motion sensor to monitor upper- extremity posture during robot-aided reaching exercise. The sensor allows the posture estimation without complicated procedures but has an inaccuracy problem such as occlusion and an unreliable segment length. Therefore, we developed a posture monitoring method, which is an analytical method without training procedure, based on the combined use of the information obtained from the sensor and the robot. Eight healthy subjects participated in the experiment with planar reaching exercise for validation. The results of joint angle estimation, high correlation coefficient (0.95 ± 0.03) and small errors (3.55 ± 0.70 deg), show that the proposed system can provide affordable upper-extremity posture estimation.**

I. Introduction

Since robots are able to provide task-specific, repetitive and intensive exercise to stroke patients, robot-aided therapy has been widely used for rehabilitation purposes [1-3]. The rehabilitation robots are classified into two types: end-effector type and exoskeleton type [1]. In reaching movement exercise for upper-extremity (UE) rehabilitation, the end-effector type robots show better clinical applicability due to their easy adaptation, simple structure, and compact size [2]. However, those robots cannot monitor the correctness of the user's (patient's) UE posture during the reaching exercise because of the lack of the user's UE joint angle information. Many studies which used the joint angle as a main feature for clinical assessments on UE motor function [4, 5] support that this lack is a key drawback of end-effector type rehabilitation robots.

In order to overcome this drawback, several studies estimated the UE kinematics by using inertial sensors or electro-goniometers attached to the user's arm [6-10]. However, the alignment of the sensors to body segments should be ensured for accurate estimation. Moreover, their required procedures have inconveniences, such as sensor attachment and initial sensor calibration. In addition, the number of sensors used would be increased for more joint angle estimations. There were attempts to estimate UE joint angles based on a simple inverse kinematics approach [11, 12]. However, those approaches required the assumptions on several strict motion/posture constraints, such as no trunk (shoulder girdle) movement and fixed shoulder abduction angle, which are different from natural reaching movement in activities of daily living [11, 12].

Since an RGB-D sensor that is vision-based and contactless type has the advantages of solving various attachment issues (i.e. misalign, time-consuming, manpower, skin artifact) and calibration issue [10-12], it could be a solution to those problems. However, the tracking accuracy of the sensor is limited when there are obstacles between the sensor and the subject [16]. In end-effector type rehabilitation robot, the users hold the handle of the robot when they perform robot-aided reaching exercise. Thus, the robot could be a significant obstacle to track their UEs using the sensor. This tracking inaccuracy can be improved by using a network of cameras with multi-camera calibration [17,18], but the calibration would be inadequate to be applied in the clinical setting. Several studies report with machine (deep) learning methods, such as convolution neural network [16,19-22], and even RGB images without depth map have been applied to estimate human posture [23-26]. Even though those studies resulted in improved tracking accuracy with appropriate training data and training processes, it still has not been verified whether those deep learning results with healthy dataset only could be effective in the rehabilitation areas with patients or not. In addition, it is difficult to collect sufficient and reliable patient dataset [5].

Therefore, we propose a novel end-effector robot system that enables the robot to monitor the user's UE posture (joint angles) during robot-aided planar reaching exercise. The proposed system contained an RGB-D sensor, and the UE joint angle estimation of the system was not based on machine learning but an analytical method that is the combined use of the RGB-D sensor information and the position information of the robot end-effector. It was based on the idea that the robot can accurately provide the position of the end-effector connected to the user during the exercise, while the RGB-D sensor cannot due to the obstacle issue of the sensor. This estimation method also included an attenuation scheme for severe inaccuracy. The proposed system was evaluated

This paper was recommended for publication by Editor Pietro Valdastri upon evaluation of the Associate Editor and Reviewers' comments. This work was supported by Basic Science Research Program through the National Research Foundation of Korea (NRF) funded by the Ministry of Education (No. 2014R1A1A2059068) and by NRF grant funded by the Korea government (MSIP) (No. 2017R1C1B2010284) (*Corresponding author: Jonghyun Kim*).

[1]Yeji Hwang and Jonghyun Kim were with the Department of Robotics Engineering, Daegu Gyeongbuk Institute of Science and Technology (DGIST), Daegu 42988, South Korea. They are now with School of Mechanical Engineering, Sungkyunkwan University, Suwon, South Korea (jonghyunkim@skku.edu).

[2]Seongpung Lee and Jaesung Hong are with the Department of Robotics Engineering, DGIST, Daegu 42988, South Korea.

Copyright ©2020 IEEE

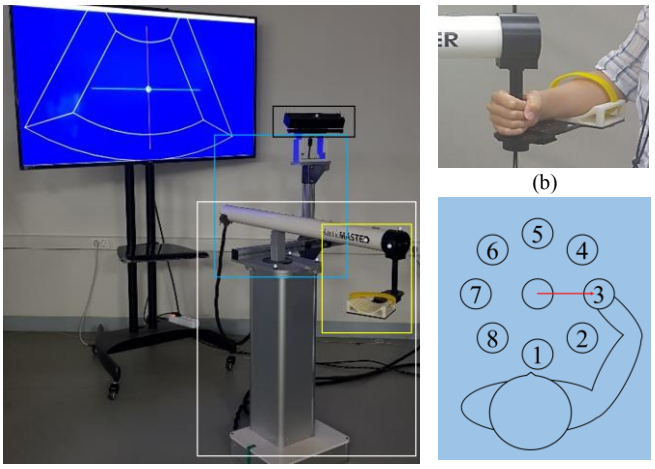

(a) (b) (c)

Fig. 1. Proposed system; (a) robot (white box), RGB-D sensor (black box), frame (blue box) and handle (yellow box); (b) custom handle; (c) planar reaching exercises and each reaching direction index

through the experiment on robot-aided planar reaching movement with eight healthy subjects.

II. Proposed Robot System

A. Proposed end-effector robot system

The proposed system, which consisted of an end-effector type robot for UE rehabilitation and an RGB-D sensor for human skeleton tracking, is shown in Fig. 1a. A commercial robot, HapticMaster (Moog FCS Robotics, The Netherlands), was used as the robot, and we used a custom handle in Fig. 1b, which was developed by our research group for planar reaching exercise by holding the user's wrist and providing gravity compensation (Fig. 1b). Note that this robot was used as a platform for robot-aided reaching exercise [27].

As mentioned, the RGB-D sensor is a promising measurement to obtain the user's joint angles based on human body skeleton tracking. We used Kinect V2 (Microsoft, USA) as the sensor. The sensor was installed in the robot for capturing the user's whole upper body by using a customized rigid frame, in order to fix the position and the orientation of the sensor (Fig. 1a).

Through the feasibility test (planar robot-aided reaching exercise) of the system, as shown in Fig. 1c, we found that the RGB-D sensor cannot be directly used for UE posture (joint angle) estimation due to the following problems.

B. Inaccuracy problem and its characteristics

In the feasibility test, the RGB-D sensor tracked the human body, but it suffered from the inaccuracy problem, such as occlusion. When the problem occurred, there was a discrepancy between the tracked body and the actual body, as shown in Fig. 2. The main reason of the inaccuracy problem is twofold; the robot arm partially blocks the sensor's view on the subject's body part, and it is difficult to distinguish between the human arm and the robot arm due to their similar depth values (distance from the sensor) under a certain upper arm posture [28,29]. Since the planar reaching exercise using the proposed system is conducted with the connection of the robot arm and the user's arm, this problem occurred more frequently than in other environments.

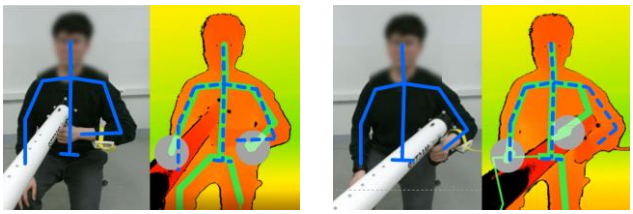

(a) (b)

Fig. 2. Inaccuracy problem (blue: expected skeleton of the actual body, green: tracked skeleton from the sensor); (a) inaccuracy of forearm; (b) inaccuracy of whole arm (severe case)

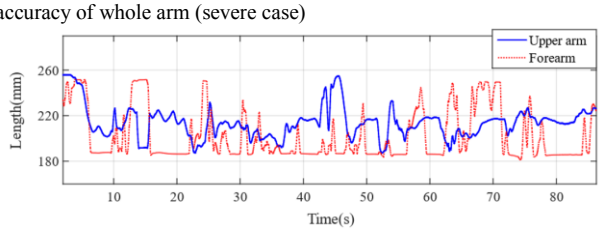

Fig. 3. Unreliable segment length during reaching exercise

The discrepancy due to the inaccuracy problem results in an unreliable segment orientation. Fig. 2a shows the unreliable forearm orientation. Since the user's forearm was connected to the handle in the proposed system, the problem majorly affected the forearm detection. However, we also found that the problem occasionally extended to the whole arm detection (severe inaccuracy). In this severe case, we also could not rely on the upper arm orientation, as shown in Fig. 2b and sudden change of UE posture occurred resulting in an abnormal angular velocity of the UE joints.

We also found that the length of the upper arm and forearm obtained from the sensor was not consistent in the feasibility test, as shown in Fig. 3. It was significantly varied and significantly shorter (up to 70 mm) than actual segment length, which can be manually measured based on bony landmarks (lateral acromion, lateral epicondyle of elbow, and wrist styloid process).

Another important characteristic of the proposed system we found was that the shoulder was free from the inaccuracy problem. The shoulder position was always stable during the test, and there was no tracking loss. Note that the tracking loss means the cases when the sensor data obtained by Kinect SDK (Microsoft, USA) gives 'inferred' or 'not tracked' tracking state.

III. Posture Monitoring Method

To solve the inaccuracy problems above, we proposed a novel analytical method to estimate the joint angle. It contains an elbow estimation method based on the combined use of kinematic data from the RGB-D sensor (shoulder position and upper-arm orientation) as well as from the robot (wrist position). For this combined use of two independent data sources, we obtained a homogeneous transformation between the sensor and the robot. Furthermore, an attenuation scheme was developed as a remedy to severe inaccuracy case, which could make the sensed upper arm orientation unreliable, in order to improve the performance of the estimation method

A. Finding homogeneous transform

In the target system, there are two coordinate systems: the robot {R} and the sensor {K}. We chose the robot coordinate

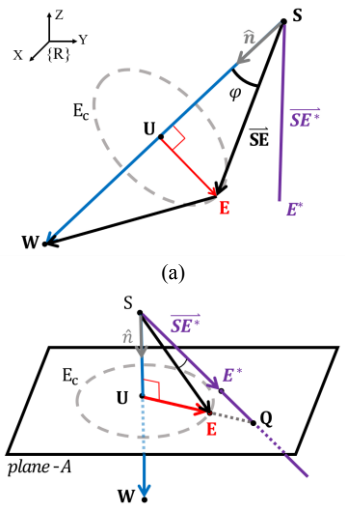

Fig. 4. Elbow position estimation method; (a) schematic diagram of the upper extremity – **S**: shoulder, **W**: wrist, $\mathbf{E}^*$: sensed elbow, **E**: estimated elbow, E_c: circle with candidates of **E**; (b) method to find one point **E** in E_c – **Q**: point where extension of $\mathbf{SE}^*$ meets plane-A. Note that orientational difference between $\mathbf{SE}^*$(sensed upper arm) and **SE** (estimated upper arm) is exaggerated for clear understanding.

as a reference of the system and obtained the coordinate relationship between {R} and {K}, (T_K^R), which represents the sensor's body tracking information based on the reference coordinate by using a well-known camera calibration with chessboard images [30] and a least-squares method [31]. It should be noted that this calculation is only required when the sensor needs to be re-installed thanks to the rigid frame in Fig. 1a.

B. Elbow position estimation method

The main idea to solve the orientation and segment length inaccuracies was to use the robot's end-point position, instead of the corrupted joint information of the RGB-D sensor. With the assumption that the end-point position is identical to the user's wrist that is connected to the robot, we can know the wrist position from the robot accurately and consistently, regardless of environmental conditions. From the characteristics of the inaccuracy problem in Section II.B, we also can trust the shoulder position obtained from the sensor. Therefore, we need a method to estimate the elbow position by combining the wrist and shoulder positions.

Fig. 4a shows the schematic diagram of the upper arm, where $\mathbf{W}=[w_x\ w_y\ w_z]^T$ and $\mathbf{S}=[s_x\ s_y\ s_z]^T$, and $\mathbf{E}^*=[e^*_x\ e^*_y\ e^*_z]^T$ denote the position vector of the wrist, shoulder, and elbow respectively. Here, $\mathbf{E}^*$ is measured by the sensor, but the proposed method is required to estimate elbow position $\mathbf{E}=[e_x\ e_y\ e_z]^T$, which would be different from $\mathbf{E}^*$ due to the previously mentioned sensor problems. Note that all vectors (**W**, **S**, $\mathbf{E}^*$ and **E**) are represented based on {R}.

As mentioned, **S** and **W** are known, and we can measure the length of the forearm (l_f) and upper arm (l_u). Therefore, the candidates of **E** can be represented as a circle (E_c), and $\mathbf{U}=[u_x\ u_y\ u_z]^T$ is defined as the center position vector of E_c (Fig. 4a). Thanks to the cosine 2nd law in a triangle **SEW**, the relative angle between **SU** and **SE** can be obtained as follows:

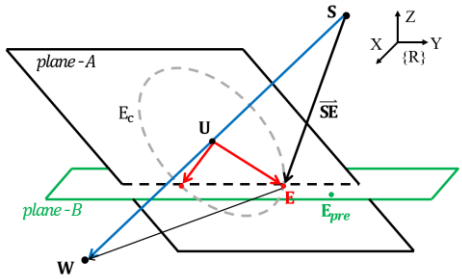

Fig. 5. Schematic diagram of attenuation scheme to find elbow during severe inaccuracy – $\mathbf{E}_{pre}$: estimated elbow **E** right before severe inaccuracy case.

$$\varphi = \arccos \frac{\left\|\overrightarrow{\mathbf{SW}}\right\|^2 + l_u^{\,2} - l_f^{\,2}}{2\left\|\overrightarrow{\mathbf{SW}}\right\| l_f} \quad . \tag{1}$$

We need to determine a point along E_c to estimate elbow position **E**. Of candidates in E_c, we chose the point that is the closest to the point $\mathbf{Q}=[q_x\ q_y\ q_z]^T$, where the extension of $\mathbf{SE}^*$ (upper arm vector measured by the sensor) meets the plane that contains E_c, as illustrated in Fig. 4b. This approach comes from the following assumption: the orientation of $\mathbf{SE}^*$ is at least reliable even under occlusion. It was due to the characteristics we found in Section II.B that the sensor mostly provides reliable upper arm orientation except for the severe inaccuracy cases.

To derive the plane equation that contains E_c, we need to know the unit vector of **SW** and a point on the plane, such as **U**. The unit vector can be defined as follows:

$$\begin{aligned}\mathbf{n} &= [n_x n_y n_z]^T \\ &= \frac{\overrightarrow{\mathbf{SW}}}{\left\|\overrightarrow{\mathbf{SW}}\right\|} = \frac{\mathbf{W}-\mathbf{S}}{\|\mathbf{W}-\mathbf{S}\|} = \frac{\mathbf{W}-T_K^R\,\mathbf{S}^K}{\|\mathbf{W}-T_K^R\,\mathbf{S}^K\|} \quad ,\end{aligned} \tag{2}$$

where $\mathbf{S}^K$ denotes the shoulder position vector described by {K}. Note that we measured $\mathbf{S}^K$ using the sensor and, $\mathbf{S}^K$ can be transformed to **S** by using T_K^R that was obtained in Section III.A. **U** can be obtained as follows:

$$\mathbf{U} = \overrightarrow{\mathbf{SU}} + \mathbf{S} = \left(l_u cos\varphi\right)\hat{\mathbf{n}} + \mathbf{S} \ . \tag{3}$$

From (2) and (3), the equation of the plane (plane-A in Fig. 4b) can be obtained as follows:

$$n_x x + n_y y + n_z z - \alpha = 0 \ , \tag{4}$$

where $\alpha = n_x u_x + n_y u_y + n_z u_z$.

To obtain **Q**, we derived the extension of $\mathbf{SE}^*$ (line) from $\mathbf{SE}^*$ (Fig. 4b), as the following equations:

$$\frac{x-s_x}{e^*_x - s_x} = \frac{y-s_y}{e^*_y - s_y} = \frac{z-s_z}{e^*_z - s_z} \ . \tag{5}$$

Hence, **Q** can be obtained by combining (4) and (5), as:

$$\begin{bmatrix} q_x \\ q_y \\ q_z \end{bmatrix} = \begin{bmatrix} n_x - \beta_x & n_y & n_z \\ n_x & n_y - \beta_y & n_z \\ n_x & n_y & n_z - \beta_z \end{bmatrix}^{-1} \begin{bmatrix} \alpha - s_x\beta_x \\ \alpha - s_y\beta_y \\ \alpha - s_z\beta_z \end{bmatrix}, \tag{6}$$

where $\beta_j = 1 / (e^*_j - s_j)$.

Since **E** is the point where **UQ** meets E_c (Fig. 4b), we can finally obtain **E** as follows:

$$\overrightarrow{\mathbf{UE}} = \left\|\overrightarrow{\mathbf{UE}}\right\| (\overrightarrow{\mathbf{UQ}} / \left\|\overrightarrow{\mathbf{UQ}}\right\|) = l_u sin\varphi (\overrightarrow{\mathbf{UQ}} / \left\|\overrightarrow{\mathbf{UQ}}\right\|), \quad (7)$$

$$\mathbf{E} = \overrightarrow{\mathbf{UE}} + \mathbf{U}. \quad (8)$$

This method aims to estimate the elbow position robustly, but its performance would deteriorate with the severe cases (significant corrupted $\mathbf{E}^*$), which makes the assumptions on the use of the upper arm ($\mathbf{SE}^*$) orientation in this subsection invalid.

C. Attenuation scheme for severe inaccuracy cases

We need an additional remedy against the severe cases. Since the characteristic of the cases is a sudden change of the upper arm posture, as mentioned in Section II.B, the angular velocity between the trunk vertical axis and the upper arm was chosen as the indicator. We detected the start of the severe case when the angular velocity was larger than a threshold that was set as 22 (°/s) based on the angular velocity under the fastest reaching task in the feasibility test and determined the end when the angular velocity was smaller than -22 (°/s).

The target task of this study is that the user holds the handle of an end-effector type robot and perform planar reaching exercise. Due to the planar motion, the variation of the vertical height of elbow (e_z) becomes negligible compared with that of e_x and e_y. Hence, during the period of the severe cases, we assumed that e_z is maintained as the z-component of the last **E** before occurring the cases ($\mathbf{E}_{pre} = [e_{pre,x}\ e_{pre,y}\ e_{pre,z}]^T$). Here, the x-y plane including $\mathbf{E}_{pre}$ (plane-B), as illustrated in Fig. 5, can be represented as follows:

$$z = e_{pre,z}. \quad (9)$$

Since E_c on plane-A is the candidate of **E**, with the e_z assumption, there are two possible **E** in the intersection between E_c (lying on plane-A) and plane-B (Fig. 5), derived by using (4) and (9) as follows:

$$n_x x + n_y y = \alpha - n_z e_{pre,z}. \quad (10)$$

As the length of **UE** is the radius of the circle, we can obtain the following equation:

$$\left\|\overrightarrow{\mathbf{UE}}\right\| = l_u \sin\varphi = \sqrt{(x-u_x)^2 + (y-u_y)^2 + (e_{pre,z} - u_z)^2} \quad (11)$$

By combining (10) and (11), we can obtain the two possible **E** ($\mathbf{E}_1$, $\mathbf{E}_2$) (Fig. 5). Of those, we opted to the closer **E** to $\mathbf{E}_{pre}$, where the following minimum is attained:

$$\min(\left\|\mathbf{E}_{\text{pre}} - \mathbf{E}_1\right\|, \left\|\mathbf{E}_{\text{pre}} - \mathbf{E}_2\right\|). \quad (12)$$

D. Upper-extremity posture monitoring

From the method above, we can obtain the upper body skeleton data (joint positions) with compensated elbow, and wrist regardless of the problems of the RGB-D sensor, as mentioned in Section II.B. Based on the position information, we can monitor the user's UE posture by using the UE joint angles estimated, which will be shown next Section. Since the target task of the estimation is planar reaching exercise using the handle (Fig. 1b), we assumed that the following movements dominantly appear: elbow flexion/extension and shoulder abduction/adduction/flexion/ extension [32].

IV. Experimental validation

A. Experiment

We conducted experiments to validate the proposed upper arm joint angle estimation system. For that, eight healthy subjects (five males; height 168.1 ± 6.6 cm, three females; height 160.7 ± 3.7 cm) participated in the experiment. All subjects performed three sessions (# of trials) of planar robot-aided reaching exercise in 8 directions, for the feasibility test (Fig. 1a). In a session, the subjects were instructed to make trunk movement during the exercise for mimicking the behaviors of stroke patients [33]. Note that the robot provided a transparent environment for the reaching exercise by using an admittance control to implement minimal impedance.

As the outcome to evaluate the accuracy of upper arm joint angle estimation, we opted to 1 elbow and 2 shoulder joint angles, as mentioned in Section III.D. The joint angles estimated by the proposed method were compared with 1) the joint angles measured by the sensor only through Kinect v2 software development kit (Microsoft, Redmond, WA, USA) (sensor only), 2) the angles estimated by simply combining the shoulder and the elbow kinematic data from the sensor and the wrist kinematic data from the robot without the proposed method in Section III (sensor+robot), and 3) the actual angles collected by a motion capture system (Bonita, Vicon, UK) with infrared markers attached to the subject's upper arm landmarks (lateral acromion, lateral epicondyle, and wrist styloid process [34]) (mocap). Note that the 'sensor+robot' result is the same as the result of 'sensor only' except wrist joint. Based on the actual angles (mocap), we calculated the correlation coefficient (CC) and the root mean square error (RMSE) for the comparison. Based on the RMSE dataset of each method, paired t-tests for elbow flexion and shoulder abduction and Wilcoxon signed-rank test for shoulder flexion were conducted to find a statistical difference in the estimation accuracy between methods. In addition, to check the possible effect of reaching direction to the posture estimation performance of the proposed method, Kruskal-Wallis H test was performed for each joint angle by using the RMSE dataset of each direction.

B. Results

Fig. 6 is the comparison results of estimated joint angles with the best and the worst subjects. In all joints, the proposed system shows the most similar joint angles to the actual angles. One can find that the simple combined use of the RGB-D sensor and the robot (sensor+robot) cannot be a solution without the proposed monitoring method, while it is better than the raw data of the sensor (sensor only) (Fig. 6).

The quantitative comparison results for all subjects were summarized in Table I. The proposed system provides the best correlated angles to the actual angles in all joints, and the RMSE results show the significantly improved accuracy of the proposed method in elbow flexion and shoulder flexion (p<0.001). There was no significant difference in the accuracy of shoulder abduction (p=0.652).

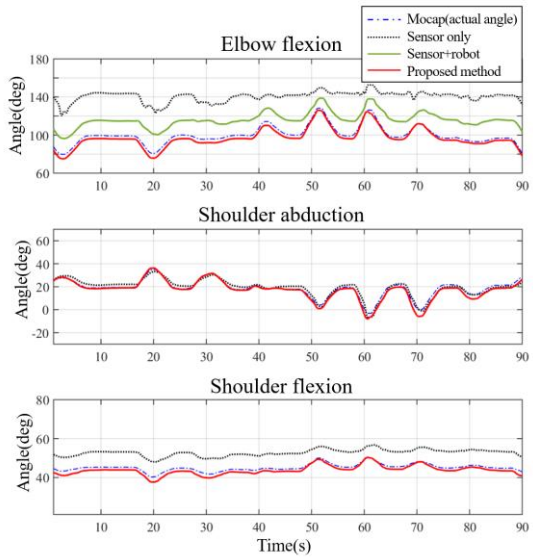

(a)

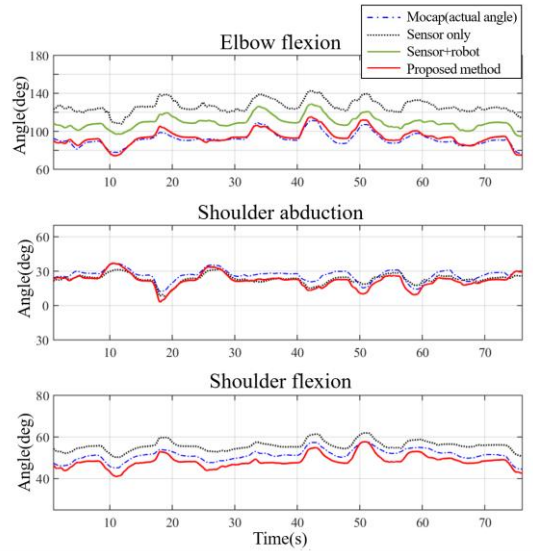

(b)

Fig. 6. Comparison of estimated joint angles with (a) the best subject and (b) the worst subject

TABLE I
COMPARISON OF JOINT ANGLE ESTIMATION ACCURACY

		Elbow angle	SHOULDER ABDUCTION	Shoulder flexion
Sensor only	CC	0.734	0.919	0.773
	RMSE (deg)	31.11	4.42	8.81
Sensor +robot	CC	0.904	0.919	0.773
	RMSE (deg)	17.688	4.42	8.81
Proposed system	CC	0.979	0.965	0.913
	RMSE (deg)	4.45	3.44	2.75

The performance of the attenuation scheme included in the monitoring method is displayed in Fig. 7, which is the result of another subject who often suffered from the severe inaccuracy cases. Note that the periods of detected severe cases were illustrated as the shaded area in Fig. 7. Despite the significant effect of the cases, the result shows that the proposed system can successfully attenuate the effect due to the scheme, and result in a noticeable correction of the

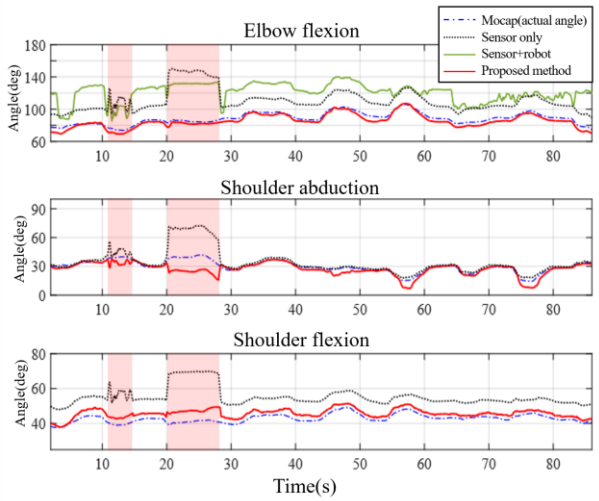

Fig. 7. Representative comparison results of estimated joint angles with attenuation scheme

TABLE II
COMPARISON OF JOINT ANGLE ESTIMATION ACCURACY UNDER SEVERE INACCURACY CASES

		Elbow angle	SHOULDER ABDUCTION	Shoulder flexion
Sensor only	CC	0.544	0.310	0.299
	RMSE (deg)	30.95	14.65	15.12
Sensor +robot	CC	0.403	0.310	0.299
	RMSE (deg)	17.58	14.65	15.12
Proposed system	CC	0.969	0.960	0.918
	RMSE (deg)	3.57	4.69	3.04

estimated UE posture (Fig. 8). Table II summarized the overall comparison results within the severe inaccuracy cases. Along with the elbow joint, the estimation accuracy of shoulder joint angles was also significantly improved. The results show that the attenuation scheme in the proposed system can robustly estimate shoulder joint angles against a highly corrupted elbow position under the severe cases.

As to the elbow flexion, there were statistically significant differences in the estimation performance between reaching directions (p=0.001): between 1 and 4 (p=0.033), 1 and 7 (p=0.015), and 2 and 7 (p=0.042). As to shoulder abduction, there was a significant difference (p=0.007): between 2 and 6 (p=0.030). On the other hand, there was no significant difference in shoulder flexion (p=0.120).

V. DISCUSSION

Although the proposed system needs an RGB-D sensor additionally, the monitoring method that also includes the attenuation scheme resulted in an affordable estimation of UE posture (joint angles), which is comparable to existing studies with inertial sensors [6-8].

Another promising benefit of the proposed system is that the monitoring method developed can be easily extended to estimate other body segments, such as the trunk. For instance, it has been reported that the patient's abnormal arm and trunk postures/motions, called compensatory movement [33], during the reaching exercise causes a side effect [34,35]. Therefore, the proposed system could be applied to classify

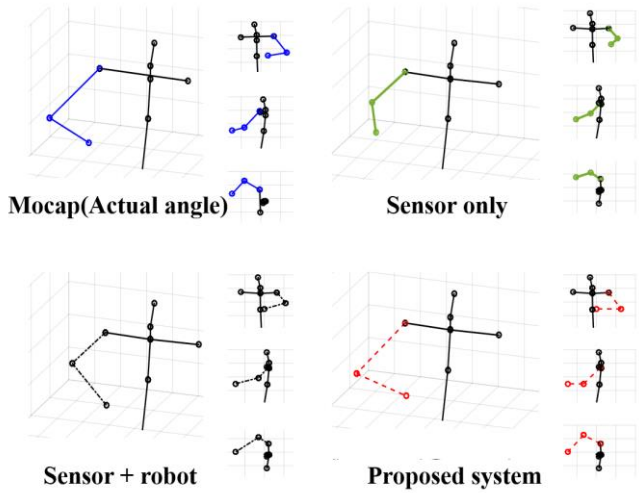

Fig. 8. Estimated upper extremity posture

and evaluate the compensatory movement by monitoring the synergy of trunk and arm motion in order to prevent the side effect without a clinician.

The statistical analysis showed that there were significant differences in the performance of the proposed UE posture monitoring method between reaching directions. However, those differences only appeared in three direction pairs in elbow flexion and one pair in shoulder abduction, and even no difference in shoulder flexion. Those results imply that the proposed method does not highly depend on reaching direction.

For the monitoring method, we assumed that the wrist motion is negligible due to the handle of the robot (Fig. 1b). During the experiments, actual wrist motion measured by motion capture system was well attenuated (about 1° on average and less than 5°), and thus it could not noticeably affect the performance of the monitoring method. Based on the characteristic of the sensor we found in Section II.B, we also assumed that the orientation of the sensed upper arm ($\mathbf{SE}^*$) is at least reliable even under occlusion. The data collected in the experiments showed the small orientational differences between the actual and the sensed upper arm (about 4°). This result quantitatively supports the assumption.

Another hypothesis we used was that the shoulder tracking of the RGB-D sensor is reliable, which is based on our findings with the proposed system. In the experiments, we also found that there was no tracking loss of shoulder joint, even with the severe inaccuracy cases. This result could indirectly support the hypothesis, but the hypothesis needs to be validated with more concrete analysis. Regarding this hypothesis, a possible limitation of the analysis in this paper is that the coordinates of the shoulder center tracked with the sensor would be different from the one achieved with the marker on the acromion.

There have been some attempts to solve the inaccuracy problem (including occlusion) of the RGB-D sensor by improving its tracking accuracy through deep learning [16,20]. However, they require training data and their target environments were quite different from the environment of this study (constituting robot as a significant obstacle). Although several attempts applied additional sensors or markers to increase the tracking accuracy [36-38], this study has used accurate and consistently available robot data to find a target-oriented solution without use of the attached sensors or markers.

Instead of the proposed elbow position estimation method, it would be possible to use a simple inverse kinematics if the elbow (and forearm) always located on the plane of planar reaching movement [11,12]. However, in contrast to the proposed method, this approach strictly requires no wrist motion, and it could cause the failure of the estimation with segment length measurement error.

In this study, the proposed system was developed based on rich experiences on the RGB-D sensor of our research group [5, 39,40] and the characteristic of the inaccuracy problem found by the feasibility test. To our knowledge, there has been no study investigating these characteristics, so this study could also contribute to developing a better combined use of the sensor and the robot.

VI. Conclusion

This paper shows that the proposed end-effector robot system can overcome the limitations of the existing end-effector robot for rehabilitation purposes: no possible monitoring of the user's UE posture correctness during reaching exercise. Thanks to the novel elbow position estimation method and the attenuation scheme against severe inaccuracy cases, the proposed robot system provides robust monitoring of UE posture without any inconvenience.

There are several directions for future research. The existing studies for general arm reconstruction used 6 or 7 degrees-of-freedom human arm model, and estimated each joint angle [7, 8], while this paper focused on the minimal required (three) joint angles for planar reaching exercise. Moreover, the scheme to attenuate the severe case was also developed based on the planar movement. Hence, we need to investigate how to extend the proposed system to the general reaching task considering more joint motions, such as forearm pronation/supination. Even though the main application of the proposed system is the reaching exercise for stroke patients, only healthy subjects participated in this study. Therefore, more diverse populations, including stroke patients who have motor disabilities, would be required to strengthen the validation of the proposed system. In addition, the target of the proposed robot system needs to be extended, such as classifying and evaluating the compensatory movement.

References

[1] W. H. Chang and Y.-H. Kim, "Robot-assisted therapy in stroke rehabilitation," *J. Stroke*, vol. 15, no. 3, p. 174-181, Sep. 2013, DOI: 10.5853/jos.2013.15.3.174.

[2] R. Riener, T. Nef, and G. Colombo, "Robot-aided neurorehabilitation of the upper extremities," *Med. Biol. Eng. Comput*., vol. 43, no. 1, p. 2-10, Jan. 2005.

[3] F. Yakub, A. Z. M. Khudzari, and Y. Mori, “Recent trends for practical rehabilitation robotics, current challenges and the future,” *Int. J. Rehabil. Res.*, vol. 37, no. 1, p. 9-21, Mar. 2014.

[4] N. Nordin, S. Q. Xie, and B. Wünsche, "Assessment of movement quality in robot- Assisted upper limb rehabilitation after stroke: A review," *J. NeuroEng. Rehabil*., vol. 11, no. 137, Sep. 2014.

[5] S. Lee, Y. S. Lee, and J. Kim, "Automated Evaluation of Upper-Limb Motor Function Impairment Using Fugl-Meyer Assessment," *IEEE Trans. Neural Syst. Rehabil. Eng*., vol. 26, no. 1, pp. 125-134, 2018.

[6] A. Bertomeu-Motos et al., "Estimation of human arm joints using two wireless sensors in robotic rehabilitation tasks," *Sensors*, vol. 15, no. 12, pp. 30571-30583, Dec. 2015.

[7] E. Papaleo et al., "Upper-limb kinematic reconstruction during stroke robot-aided therapy," *Med. Biol. Eng. Comput*., vol. 53, no. 9, pp. 815-828, Sep. 2015.

[8] A. Bertomeu-Motos et al., " Human arm joints reconstruction algorithm in rehabilitation therapies assisted by end-effector robotic devices." *Journal of neuroengineering and rehabilitation*, vol. 15, no. 1, pp. 10, 2018.

[9] P. T. Wang, C. E. King, A. H. Do, and Z. Nenadic, “A durable, low-cost electrogoniometer for dynamic measurement of joint trajectories,” *Med. Eng. Phys.,* vol. 33, no. 5, pp. 546-552, Jan. 2011.

[10] Peternel, Luka, et al. "Towards ergonomic control of human-robot co-manipulation and handover." *2017 IEEE-RAS 17th International Conference on Humanoid Robotics (Humanoids).* IEEE, 2017.

[11] Sukal, Theresa M., Michael D. Ellis, and Julius PA Dewald. "Shoulder abduction-induced reductions in reaching work area following hemiparetic stroke: neuroscientific implications." *Experimental brain research* 183.2 (2007): 215-223.

[12] Ellis, Michael D., et al. "Augmenting clinical evaluation of hemiparetic arm movement with a laboratory-based quantitative measurement of kinematics as a function of limb loading." *Neurorehabilitation and neural repair* 22.4 (2008): 321-329.

[13] B. Bouvier, S. Duprey, L. Claudon, R. Dumas, and A. Savescu, “Upper limb kinematics using inertial and magnetic sensors: comparison of sensor-to-segment calibrations," *Sensors*, vol. 15, no. 8, pp. 18813–18833, July. 2015.

[14] X. Robert-Lachaine, H. Mecheri, C. Larue, and A. Plamondon, “Validation of inertial measurement units with an optoelectronic system for whole-body motion analysis,” *Med. Biol. Eng. Comput*., vol. 55, no. 4 pp. 609–619. Apr. 2017.

[15] L. Vargas–Valencia, A. Elias, E. Rocon, T. Bastos–Filho, and A Frizera, “An IMU–to–body alignment method applied to human gait analysis,” *Sensors*, vol. 16, no. 12, pp.2090–2107. Dec. 2016.

[16] C. Zimmermann, T. Welschehold, C. Dornhege, W. Burgard, and T. Brox, “3d human pose estimation in rgbd images for robotic task learning,” *In 2018 IEEE International Conference on Robotics and Automation (ICRA)*, pp. 1986-1992.

[17] Munaro, Matteo, Filippo Basso, and Emanuele Menegatti. "OpenPTrack: Open source multi-camera calibration and people tracking for RGB-D camera networks." *Robotics and Autonomous Systems* 75 (2016): 525-538.

[18] Pfister, Alexandra, et al. "Comparative abilities of Microsoft Kinect and Vicon 3D motion capture for gait analysis." *Journal of medical engineering & technology* 38.5 (2014): 274-280.

[19] Martínez-González, Ángel et al. “Real-time Convolutional Networks for Depth-based Human Pose Estimation.” *2018 IEEE/RSJ International Conference on Intelligent Robots and Systems (IROS)*, pp. 41-47.

[20] Li, Ruotong et al. “Constraint-Based Optimized Human Skeleton Extraction from Single-Depth Camera.” *Sensors*, vol. 19, no. 11, pp. 2604, Jun. 2019.

[21] Vasileiadis, Manolis, C. S. Bouganis, and D. Tzovaras. "Multi-person 3D pose estimation from 3D cloud data using 3D convolutional neural networks." *Computer Vision and Image Understanding*, vol. 185, pp. 12-23, Aug. 2019.

[22] FANG, Hao-Shu, et al. “Rmpe: Regional multi-person pose estimation.” *In: Proceedings of the IEEE International Conference on Computer Vision.* 2017. p. 2334-2343.

[23] R. Alp Güler, N. Neveroca, and I. Kokkinos, “Densepose: Dense human pose estimation in the wild,” *In: Proceedings of the IEEE Conference on Computer Vision and Pattern Recognition.* 2018. pp. 7297-7306.

[24] D. Tome, C. Russell, and L Agapito, “Lifting from the deep: Convolutional 3d pose estimation from a single image,” *In: Proceedings of the IEEE Conference on Computer Vision and Pattern Recognition*. 2017. pp. 2500-2509.

[25] Z. Cao, T Simon, S. E. Wei, and Y. Sheikh, ”Realtime multi-person 2d pose estimation using part affinity fields.” *In: Proceedings of the IEEE Conference on Computer Vision and Pattern Recognition.* 2017. pp. 7291-7299.

[26] Z. Cao, G. Hidalgo, T. Simon, S.-E. Wei, Y. Sheikh, “OpenPose: realtime multi-person 2D pose estimation using Part Affinity Fields” arXiv preprint arXiv:1812.08008, 2018.

[27] S. V. Adamovich, G. G. Fluet, A. S. Merians, A. Mathai, and Q. Qiu, "Incorporating haptic effects into three-dimensional virtual environments to train the hemiparetic upper extremity," *IEEE Trans. Neural Syst. Rehabil. Eng,* vol. 17, no. 5, pp. 512-520, Oct. 2009.

[28] Š. Obdržálek, G. Kurillo, F. Ofli, R. Bajcsy, E. Seto, H. Jimison, and M. Pavel, "Accuracy and robustness of Kinect pose estimation in the context of coaching of elderly population*," 2012 Annual International Conference of the IEEE Engineering in Medicine and Biology Society,* pp. 1188-1193.

[29] J. Han, L. Shao, D. Xu, and J. Shotton, "Enhanced computer vision with Microsoft Kinect sensor: A review," *IEEE T. Cybern.*, vol. 43, no. 5, pp. 1318-1334, Oct. 2013.

[30] M. Shah, "Solving the robot-world/hand-eye calibration problem using the kronecker product," *J. Mech. Robot*., vol. 5, no. 3, 2013.

[31] Z. Zhang, "A flexible new technique for camera calibration," *IEEE Trans. Pattern Anal. Mach. Intell.*, vol. 22, no. 11, pp. 1330-1334, Nov. 2000.

[32] M. C. Cirstea and M. F. Levin, "Compensatory strategies for reaching in stroke," *Brain*, vol. 123, no. 5, pp. 940-953, May. 2000.

[33] Taati, Babak, et al. "Vision-based categorization of upper body motion impairments and post-stroke motion synergies." *International Journal on Disability and Human Development* 13.3 (2014): 343-348.

[34] M. F. Levin, D. G. Liebermann, Y. Parmet, and S. Berman, "Compensatory Versus Noncompensatory Shoulder Movements Used for Reaching in Stroke," *Neurorehabil. Neural Repair*, vol. 30, no. 7, pp. 635-646, Aug. 2016.

[35] Y. X. Zhi, M. Lukasik, M. Li, E. Dolatabadi, R. H. Wang, and B. Taati, "Automatic Detection of Compensation during Robotic Stroke Rehabilitation Therapy," *IEEE J. Transl. Eng. Health Med*.-JTEHM, , vol. 6, 2018.

[36] Du, Yi-Chun, et al. "An IMU-compensated skeletal tracking system using Kinect for the upper limb." *Microsystem Technologies* 24.10 (2018): 4317-4327.

[37] A. Timmi et al. "Accuracy of a novel marker tracking approach based on the low-cost microsoft kinect v2 sensor." *Medical engineering & physics* 59 (2018): 63-69.

[38] H. Tannous et al. "A new multi-sensor fusion scheme to improve the accuracy of knee flexion kinematics for functional rehabilitation movements." *Sensors* 16.11 (2016): 1914.

[39] P. Otten, J. Kim, and S. H. Son, "A framework to automate assessment of upper-limb motor function impairment: A feasibility study," *Sensors*, vol. 15, no. 8, pp. 20097-20114, Aug. 2015.

[40] J. Kim, A. Gravunder, and H. S. Park, "Commercial Motion Sensor Based Low-Cost and Convenient Interactive Treadmill," *Sensors*, vol. 15, no. 9, pp. 23667-23683, Sep. 2015.